Analysis of Damped Vibration by MSKE Method for Structures Having Porous Layer Sandwiched by Double Walls with Acoustic Black Hole in Cover Plate

Takao Yamaguchi[1,a,*], Chihiro Kamio[1,b], Yuta Hisamura[2,c]

[1]Gunma University, 1-5-1 Tenjin-cho, Kiryu, Gunma, 376-8515 Japan

[2]Graduate School of Gunma University, 1-5-1 Tenjin-cho, Kiryu, Gunma, 376-8515 Japan

*Corresponding author

[a]<yamagme3@gunma-u.ac.jp>, [b]<chihiro.kamio@gunma-u.ac.jp>

Keywords: acoustic black hole, finite element method, damping, porous layer, vibration transmission.

Abstract. Vibration suppression is an important technology both industrially and environmentally to realize a comfort industrial product with a safe structure. In this paper, we carried out numerical simulation of damped vibration for a structure having a porous material sandwiched by double walls. The cover plate in double walls has a Krylov type acoustic black hole. All edges where the black hole exists, have free boundaries. Damping material is laminated on the surface of the black hole. Numerical analysis is performed to clarify changes of vibration reduction and vibration transmission from the base plate to the cover plate due to the acoustic black hole using FEM and MSKE method proposed by Yamaguchi et al.

1. Introduction

Vibration damping is an important technology from an industrial and environmental perspective to realize industrial products with safe and comfort. In automobiles and buildings, double walls with a porous layer are sometimes used to decrease vibration and noise. Mironov [1] proposed a vibration damping method called acoustic black hole. Furthermore, Krylov [2], [3] et al. have proposed a structure with damping material on the surface of the steel plate in the black hole area. And, this increases damping effects. In our research, we deal with a model that has an acoustic black hole with a damping layer on a cover plate in a double walls structure. There exists a porous layer sandwiched by the walls. We modeled this using FEM and numerically analyzed vibration of these structures using MSKE method proposed by Yamaguchi et al. [4]. We investigated changes in the vibration reduction characteristics and vibration transmission characteristics due to the acoustic black hole.

Mironov [1] studied vibration propagations of bending waves in a flat plate having an edge where the thickness of the plates decreasing to the edge as a quadratic function x^2 of the distance x from the boundary. Due to the black hole, it is difficult that the bending waves reflect at the edge. Mironov called this structure as acoustic black hole. But, to obtain sufficient vibration reduction effects, it is necessary that the length of the edge is enough long. At the edge, the thickness is too thin to compensate the strength of the structures. To improve this, Krylov proposed to modify the Mironov's acoustic black hole [2], [3] by cutting off the edge practically as finite length. Further, Krylov added a thin viscoelastic damping layer on the edge. According to Oberst theory [7], vibration damping effects of a straight metal beam covered with a viscoelastic layer are proportional to (thickness of the damping layer/ thickness of the metal beam)^2. Thus, high efficient damping effects appear when a viscoelastic damping layer is covered on the edge in the black hole because of thin thickness around the black holes. We introduced this acoustic black hole to the cover plate (Fig.1) in the double walls. And we evaluate its effect for vibration reduction.

2. Calculation Details

Figure 1 shows the calculation model with acoustic black hole in the cover plate.

A porous layer is sandwiched between a steel base plate and a steel cover plate. The thickness of the porous material is 11.25[mm] and the thickness of the cover plate is 5.04[mm]. The thickness of the base plate is also 5.04[mm]. The side length of the base plate is 280 x 195[mm]. The long side direction of the plate is the x-axis, the height direction is the y-axis, and the short side direction is the z-axis. The model without acoustic black hole is called as model1 in this paper.

Next, a structure of the Krylov type acoustic black hole [2], [3] with a length of 45 [mm] is attached to one short side of the cover plate of model 1, and a damping material with a thickness of 1 [mm] is layered on the top of the acoustic black hole. This is model 2 with acoustic black hole in this paper. Here, The reduction function of the thickness $h(x)$ for the part of the black hole is $h(x)=\varepsilon x^{m}$ (m=2.2). This function and the geometry of the cover plate are same as the Krylov's experiment [3]. The boundary conditions are set as the entire peripheries of both the base plate and cover plate are free. In addition, the edges of the porous material layer are set as rigid wall, and the particle displacement inside the porous material and the displacement of the both plates (base and cover plates) are continuous only in the normal direction to the boundary surface. The excitation position is the back side of the steel base plate, and is the point shifted 5 mm from the center of the base plate in the z-axis direction. This coordinate is (x, y, z) =(162.5, 0, 102.6). The excitation direction is the y-axis direction, and the waveform of the excitation is white noise.

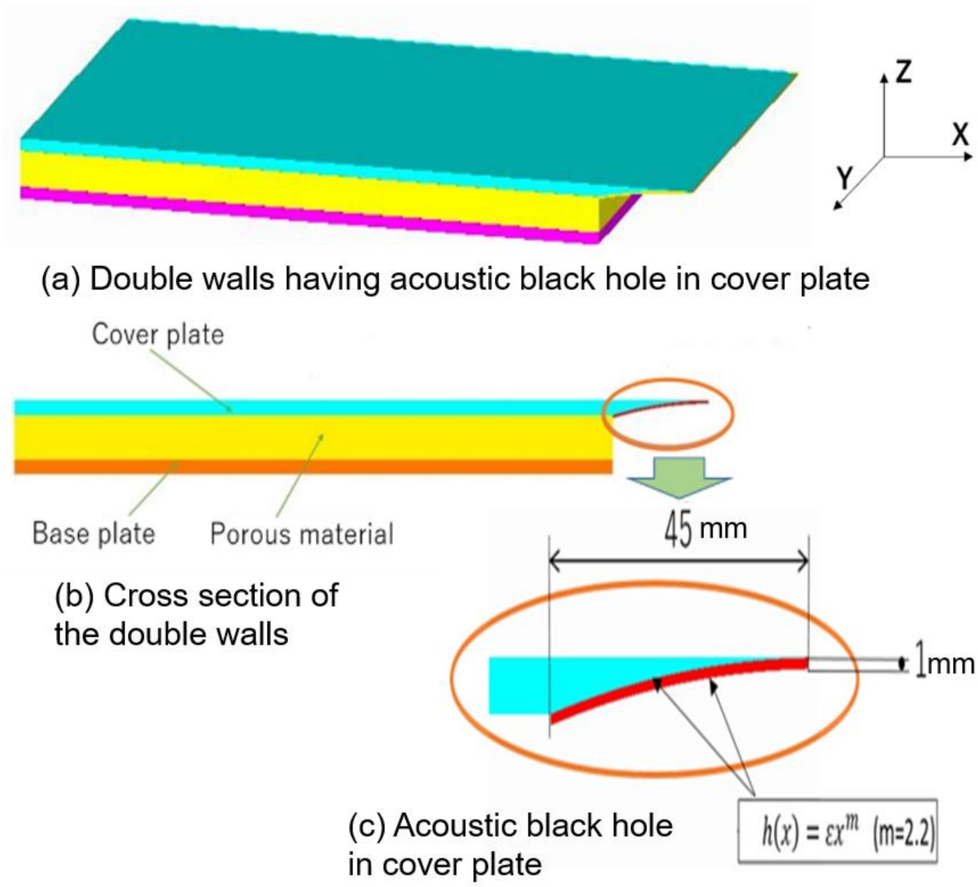

Fig. 1. FEM model including cover plate with acoustic black hole having damping layer (model2).

3. Numerical Method [4]-[6]

3.1 Discrete Equations in Porous Layer

For the internal air in the porous layer, we use a finite element model as shown in this section. Considering periodic oscillation and infinitesimal amplitude, the equations of motion can be written for inviscid compressive perfect fluid as follows.

$$-\mathrm{grad}\, p = -\rho_e \omega^2 \{u_f\} \tag{1}$$

The continuity equation is shown as:

$$p = -E_e \mathrm{div}\{u_f\} \tag{2}$$

$\{u_f\}$ is the particle displacements vector. p denotes sound pressure. ρ represents the effective density of the internal air. E represents the modulus of volume elasticity of the internal air. ω is the angular frequency. Here, the particle displacements $\{u_f\}$ are chosen as unknowns [4]-[6] by eliminating the sound pressure p in equations. (1) and (2). The displacement is chosen as the common unknown variable for the double walls structure with acoustic black hole.

We approximate the relation between $\{u_f\}$ and particle displacement vectors $\{u_{fe}\}$ at nodal points in the element as

$$\{u_f\} = [N_f]^T \{u_{fe}\} \tag{3}$$

Where, $[N_f]^T$ represents a matrix comprised of proper shape functions.

From equations (1), (2) and (3), the strain energy, kinetic energy, and external work can be determined. After applying the Minimum Energy Principle, the following equations are obtained.

$$\left([K]_{fe} - \omega^2 [M]_{fe}\right)\{u_{fe}\} = \{f_{fe}\} \tag{4}$$

$$[K]_{fe} = E_e \left[\widetilde{K}\right]_{fe} \tag{5}$$

$$[M]_{fe} = \rho_e \left[\widetilde{M}\right]_{fe} \tag{6}$$

E_e and ρ_e show the volume elasticity and the effective density in the domain of the elements, respectively. $[K]_{fe}$ and $[M]_{fe}$ show the element stiffness matrix and the element mass matrix, respectively. $\left[\widetilde{K}\right]_{fe}$, $\left[\widetilde{M}\right]_{fe}$ show the matrix including the shape functions and their derivatives. $\{f_{fe}\}$ is the nodal force vector.

We utilize the following model having the complex effective density ρ_e^* and complex volume elasticity E_e^*, for damped sound fields inside porous materials [8], [4]-[6]:

$$\rho_e \Rightarrow \rho_e^* = \rho_{eR} + \boldsymbol{j}\rho_{eI} \tag{7}$$

$$E_e \Rightarrow E_e^* = E_{eR} + \boldsymbol{j}E_{eI} \tag{8}$$

Where, $\boldsymbol{j}$ is the imaginary unit. ρ_{eR} and ρ_{eI} are the real and imaginary parts of ρ_e^*, respectively. E_{eR} and E_{eI} show the real and imaginary parts of E_e^*, respectively. We verified that this model is suitable for fibrous materials in cars [4]-[6]. We assumed the elastic waves through the resin fiber of the porous materials can be neglected.

Element mass matrix $[M]_{fe}$ can be written by substituting equation (7) into equation (6).

$$[M]_{fe} = [M_R]_{fe}\left(1 + \boldsymbol{j}\chi_{fe}\right) \tag{9}$$

$$\chi_{fe} = \rho_{eI}/\rho_{eR} \tag{10}$$

$[M_R]_{fe}$ is the real part of the element mass matrix $[M]_{fe}$. ρ_{eI} is the imaginary part of the effective density. $\chi_{fe} = \rho_{eI}/\rho_{eR}$ shows the damping effect originated from flow resistance.

Substituting Eqn.(8) into Eqn.(5), the following element stiffness matrix $[K]_{fe}$is given.

$$[K]_{fe} = [K_R]_{fe}\left(1 + \boldsymbol{j}\eta_{fe}\right) \tag{11}$$

$$\eta_{fe} = E_{eI}/E_{eR} \tag{12}$$

In equation (11), $[K_R]_{fe}$ shows the real part of the element stiffness matrix $[K]_{fe}$. In equation (12), η_{fe} shows the damping effect due to hysteresis between pressure and volume strain in the porous materials.

Both the element mass matrix $[M_R]_{fe}$ and the element stiffness matrix $[K]_{fe}$ for internal gas in the porous materials have complex quantities.

The complex effective density is ρ_{eR} = 1.40kg/m^3, χ_{fe} = -0.500. And the complex volume elasticity is E_{eR} = 1.19×10^5 N/m^2, η_{fe} = 0.100. For the porous layer in the double-walled structures, the isoparametric hexagonal elements [9] are used.

3.2 Equation for Vibration of Solid Bodies with Damping in the Double Walls

We used discretized equations shown in the following equations from equations (13) to (15) for vibration of the base plate and the cover plate with the acoustic black hole. For the viscoelastic layer on the acoustic black hole, we use the same model. These models are considered as conventional linear finite element model with hysteresis damping.

$\{u_s\}$ shows the displacement vector for the solid bodies. Using the matrix comprised of shape functions$[N_s]^T$, the relation between the displacements $\{u_{se}\}$ at nodal points and the displacement vector $\{u_s\}$ in an element for the solid bodies are approximated as:

$$\{\boldsymbol{u_s}\} = [\boldsymbol{N_s}]^{\boldsymbol{T}}\{\boldsymbol{u_{se}}\} \tag{13}$$

Strain energy, kinetic energy, and external work are determined, and then, by applying the agrange equation, the following expressions are given.

$$([K]_{se} - \omega^2[M]_{se})\{u_{se}\} = \{f_{se}\} \tag{14}$$

$$[K]_{se} = [K_R]_{se}(1 + \boldsymbol{j}\eta_{se}) \tag{15}$$

$[K]_{se}$ and $[M]_{se}$ represent the element stiffness matrix and element mass matrix, respectively. $\{f_{se}\}$ shows the nodal force vector in an element e for the solid bodies. The element stiffness matrix

$[K_R]_{se}$ in equation (15) has complex quantities in equation (14). $[K_R]_{se}$ shows the real part of element stiffness matrix for the solid bodies. η_{se} shows the material loss factor corresponding to each element e.

For the viscoelastic materials and the elastic materials, the isoparametric hexahedral elements [9] are mainly used with the non-conforming modes. For the viscoelastic damping material, the storage modulus of elasticity is 1.6×10^9 N/m^2, the mass density is 1.9×10^3 kg/m^3 and the material loss factor η_{se} is 0.5.

3.3 Discrete Equations for the Global System for the Double Walls with Acoustic Black Hole

All elements for the porous layer and the base plate and the cover plate in the double walls having the acoustic black hole are superposed by using equations from (4) to (15). At boundaries between the porous layer and the solid bodies (i.e. the cover plate and the base plate), normal components of the displacements to the boundaries are continuous. Tangential components of the displacements along the boundaries are independent. From these conditions, the following equation is given.

$$([K]_a - \omega^2[M]_a)\{u_a\} = \{f_a\} \tag{16}$$

Where, $\{f_a\}$ shows the nodal force vector and $\{u_a\}$ shows the nodal displacement vector. $\{u_a\}$ is comprised of $\{u_{fe}\}$ and $\{u_{se}\}$. $[K]_a$ contains $[K]_{fe}$ and $[K]_{se}$, while $[M]_a$ includes $[M]_{fe}$ and $[M]_{se}$.

3.4 Expressions for Modal Damping by Using MSKE Method [4]-[6]

By ignoring the external force vector from equation (16), we can obtain the following complex eigenvalue problem:

$$\sum_{e=1}^{e_{\max}}([K_R]_e(1+\boldsymbol{j}\eta_e) - \left(\omega^{(i)}\right)^2(1+\boldsymbol{j}\eta_{\text{tot}}^{(i)})[M_R]_e(1+\boldsymbol{j}\chi_e))\{\phi^{(i)^*}\} = \{0\} \tag{17}$$

Where, superscript (i) represents the i-th eigenmode. $\left(\omega^{(i)}\right)^2$ shows the real part of complex eigenvalue. $\{\phi^{(i)^*}\}$ shows the complex eigenvector and $\eta_{\text{tot}}^{(n)}$ represents the modal loss factor. $[K_R]_e$ shows the real part of element stiffness matrix. $[M_R]_e$ denotes the real part of element stiffness matrix.

Next, the following parameters β_{se} and β_{ke} are introduced:

$$\beta_{se} = \frac{|\eta_e|}{\eta_{\max}},\ \ \beta_{se} \leqq 1,\ \beta_{ke} = \frac{|\chi_e|}{\eta_{\max}},\ \ \beta_{ke} \leqq 1 \tag{18}$$

$\eta_{\max}$ shows the maximum value among the elements' material loss factors η_e and χ_e, (e=1,2, 3, ..., $e_{\max}$). Under assumption of $\eta_{\max} \ll 1$, solutions of equation (17) can be expanded using a small parameter $\mu = \boldsymbol{j}\eta_{\max}$:

$$\{\phi^{(i)^*}\} = \{\phi^{(i)}\}_0 + \mu\{\phi^{(i)}\}_1 + \mu^2\{\phi^{(i)}\}_2 + \cdots\cdots \tag{19}$$

$$\left(\omega^{(i)}\right)^2 = (\omega_0{}^{(i)})^2 + \mu^2(\omega_2{}^{(i)})^2 + \mu^4(\omega_4{}^{(i)})^2 + \cdots\cdots \tag{20}$$

$$\boldsymbol{j}\eta_{\text{tot}}{}^{(i)} = \mu\eta_1{}^{(i)} + \mu^3\eta_3{}^{(i)} + \mu^5\eta_5{}^{(i)} + \cdots\cdots \tag{21}$$

In the equations, under conditions of $\beta_{se} \leqq 1$, $\beta_{ke} \leqq 1$ and $\eta_{\max} \ll 1$, we can get $\eta_{\max}\beta_{se} \ll 1$ and $\eta_{\max}\beta_{ke} \ll 1$. Therefore, $\mu\beta_{se}$ and $\mu\beta_{ke}$ can be considered as small parameter like μ. In these equations, $\{\phi^{(i)}\}_0$, $\{\phi^{(i)}\}_1$, $\{\phi^{(i)}\}_2$, ... and $(\omega_0{}^{(i)})^2$, $(\omega_2{}^{(i)})^2$, $(\omega_4{}^{(i)})^2$,...and $\eta_1{}^{(i)}$, $\eta_3{}^{(i)}$, $\eta_5{}^{(i)}$, ... have real quantities.

By substituting these equations from equations (19) to (21) into equation (17), the following equation can be obtained:

$$\eta_{\mathrm{tot}}{}^{(i)} = \eta_{se}{}^{(i)} - \eta_{ke}{}^{(i)} \tag{22}$$

$$\eta_{se}{}^{(i)} = \sum_{e=1}^{e_{max}} \left(\eta_e S_{se}{}^{(i)}\right) ,S_{se}{}^{(i)} = \{\phi^{(i)}\}_0{}^T [K_R]_e \{\phi^{(i)}\}_0 / \sum_{e=1}^{e_{\max}} \{\phi^{(i)}\}_0{}^T [K_R]_e \{\phi^{(i)}\}_0$$

$$\eta_{ke}{}^{(i)} = \sum_{e=1}^{e_{max}} (\chi_e S_{ke}{}^{(i)}) ,S_{ke}{}^{(i)} = \{\phi^{(i)}\}_0{}^T [M_R]_e \{\phi^{(i)}\}_0 / \sum_{e=1}^{e_{\max}} \{\phi^{(i)}\}_0{}^T [M_R]_e \{\phi^{(i)}\}_0$$

For the expressions, modal loss factor $\eta_{\mathrm{tot}}{}^{(i)}$ can be computed using $\eta_{se}{}^{(i)}$ and $\eta_{ke}{}^{(i)}$. $\eta_{se}{}^{(i)}$ can be determined using share $S_{se}{}^{(i)}$of strain energy of each element to total strain energy and material loss factors η_e of each element e. $\eta_{ke}{}^{(i)}$ can be determined using share $S_{ke}{}^{(i)}$of kinetic energy of each element to total kinetic energy and material loss factors χ_e of each element e

While the material loss factors η_e are related with hysteresis damping in the relation between stress and strain, the material loss factors χ_e are related with flow resistance. The eigenmodes $\{\phi^{(i)}\}_0$ in equation (22) has real quantity. Thus, the eigenmodes can be calculated by solving real eigenvalue problem, which corresponds to the equation by deleting damping parameters in equation (17). We named the equation (22) as Modal Strain and Kinetic Energy Method (MSKE method) [4]-[6]. This method corresponds to the extended version of Modal Strain Energy Method (MSE method) for structures having elastic bodies with viscoelastic bodies.

3.5 Computation of Vibration Responses Using MSKE Method [4]-[6]

Under input force, acceleration $\{A_{out}\}$ as vibration responses in the structures are calculated using the modal parameters and modal damping from MSKE method in Sec.3.4 as follows.

$$\{A_{out}\} = \sum_{i=1}^{max} \frac{-\omega^2 \left\{\phi_{in}^{(i)}\right\}^t \{F_{in}\} \left\{\phi_{out}^{(i)}\right\}}{m^{(i)}\left[\left(\omega^{(i)}\right)^2 - \omega^2 + \boldsymbol{j}\left(\omega^{(i)}\right)^2 \eta_{se}^{(i)} - \boldsymbol{j}\omega^2 \eta_{ke}^{(i)}\right]} \tag{23}$$

$\{F_{in}\}$ is the external force vector at the excitation points, $\left\{\phi_{in}^{(i)}\right\}$ is the *i*-th eigenmode at the excitation points, $\left\{\phi_{out}^{(i)}\right\}$ is the *i*-th eigenmode at the observation points, $m^{(i)}$ is the *i*-th modal mass.

4. Analysis Results and Considerations

The average acceleration levels of the entire surface of the base and cover plates are clarified into 1/3 octave bands to evaluate the vibration reduction.

4.1 Average Acceleration Level of Base Plate

Figure 2 represents vibration acceleration levels $|A_{\mathrm{base}}|_{\mathrm{av}}$ of the base plate in the double walls with / without the acoustic black hole. This value $|A_{\mathrm{base}}|_{\mathrm{av}}$ is averaged over all nodes in the base plate. In Fig.2, 0dB means 1m/sec.^{2}/N. From Fig.2, it can be seen that model 1 (no acoustic black hole) has the same amplitude level as model 2 (acoustic black hole with damping material layer) after the 500Hz band.

Since both models have the same flat base plates with no acoustic black hole, it is thought that they are not affected by attenuation by the acoustic black hole in the cover plate.

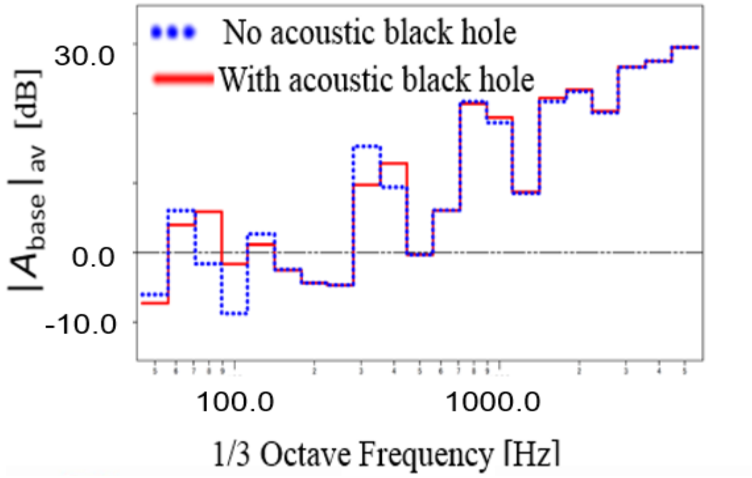

Fig. 2. Acceleration level of base plate.

4.2 Average Acceleration Level of Cover Plate

Figure 3 shows vibration acceleration levels $|A_{cover}|_{av}$ of the cover plate in the double walls with / without the acoustic black hole. This value $|A_{cover}|_{av}$ is averaged over all nodes in the cover plate. In Fig.3, 0dB means 1m/sec.^{2}/N, too.

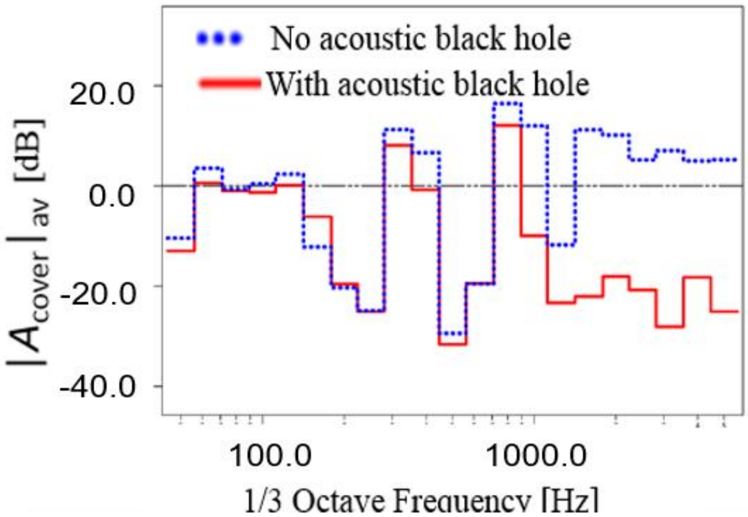

Fig. 3. Acceleration level of cover plate.

From Fig.3, it can be seen that $|A_{cover}|_{av}$ of model 2 (acoustic black hole, with damping material) is smaller than $|A_{cover}|_{av}$ of model 1 (no acoustic black hole) in the 315 Hz, 400 Hz bands and after 800 Hz band.

4.3 Evaluation of Vibration Transmission Properties for the Double Walls Including Acoustic Black Hole

Figure 4 shows vibration transmission $|A_{\text{base to cover}}|_{av}$ from the base plate and the cover plate. In Fig.4, positive value in $|A_{\text{base to cover}}|_{av}$ means magnification of vibration propagation, while negative value means that we can get vibration isolation. We can observe large effects for the isolation in the higher frequency region than 800Hz band due to the presence of the acoustic black hole in the cover plate.

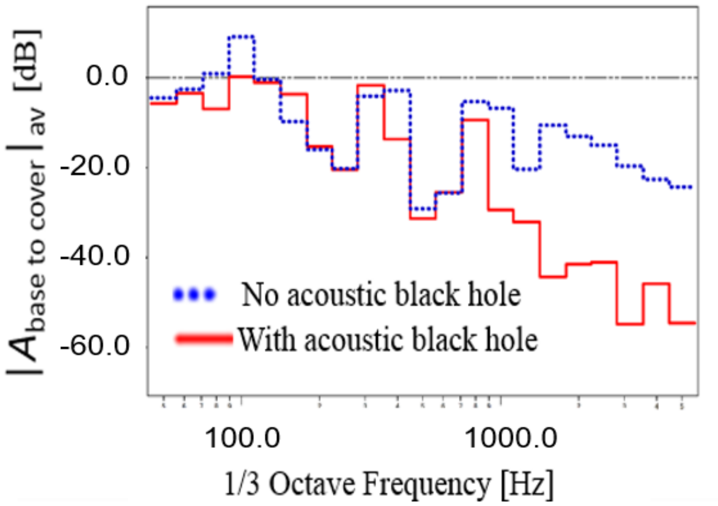

Fig. 4. Vibration transmission level from base plate to cover plate (Effects of acoustic black hole in the cover plate).

4.4 Eigenmodes of Structures with Acoustic Black Hole

Deformation distributions of the structure with acoustic black hole were visualized as eigenmodes using FEM.

Figure 5 shows typical examples of eigenmodes having dominant large deformations in the area where the acoustic black hole exists. As can be seen, these modes can have large modal loss factors. On the other hand, Figure 6 represents typical examples of eigenmodes having relatively small non-dominant deformations in the area where there is acoustic black hole. As can be seen, these modes tend to have small modal loss factors.

From these results, it can be seen that damping effects become larger, when the deformations in the area of acoustic black hole becomes larger.

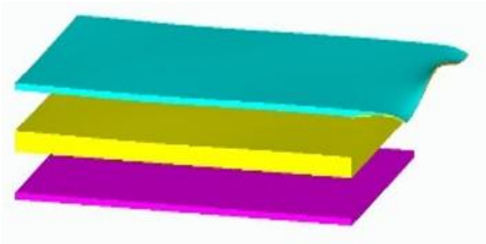

(a) Eigenmode under f [Hz]=1790, η_{tot} [-]= 0.0482

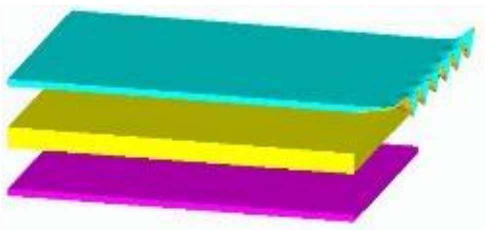

(b) Eigenmode under f [Hz]=4590 , η_{tot} [-]= 0.327

Fig. 5. Typical examples of eigenmodes (Dominant large deformations in acoustic black hole: high damping).

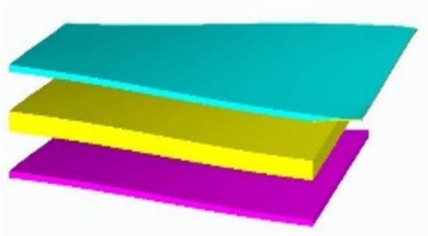

(a) Eigenmode under
f [Hz]=310, η_{tot} [-]= 0.00161

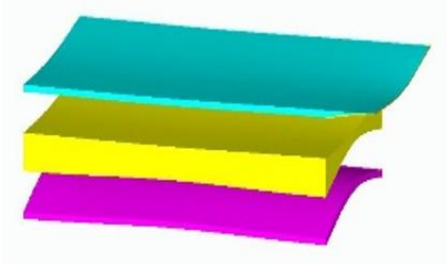

(b) Eigenmode under
f [Hz]=748 , η_{tot} [-]= 0.00257

Fig. 6. Typical examples of eigenmodes (Relatively small deformations in acoustic black hole: low damping).

5. Conclusion

Double walls having an acoustic black hole with a damping material layer on the cover plate was numerically analyzed using FEM and MSKE method, and the vibration reduction characteristics and vibration transmission characteristics were clarified. All edges around both the base plate and cover plate, were free. A porous layer was sandwiched between the plates. The base plate in the double walls was excited at a point.

For the cover plate, the average acceleration level became smaller after the middle frequency band, when there exists acoustic black hole in the cover plate. Damping effects due to the black hole appears when vibrations were transmitted from the base plate to the acoustic black hole through the cover plate.

For the base plate, there was no difference in the average acceleration level between the models with/without the black hole in the mid-frequency range and beyond. This is due to the absence of the acoustic black hole.

It is found that damping effects become larger, when the deformations in the area of acoustic black hole in the cover plate becomes larger.

References

[1] M.A. Mironov, “Propagation of a flexural wave in a plate whose thickness decreases smoothly to zero in a finite interval”, ***Soviet Physics-Acoustics*** Vol.34, pp.318–319, 1988.

[2] V.V. Krylov, F.J.B.S. Tilman, “Acoustic ‘black holes’ for flexural waves as effective vibration dampers”, ***Journal of Sound and Vibration***, Vol.274 (3–5), pp.605–619,2004.

[3] V.V. Krylov, V. Kralovic, D.J. O’Boy, “Damping of flexural vibrations in rectangular plates using the acoustic black hole effect”, ***Journal of Sound and Vibration***, Vol.329, pp.4672-4688, 2010.

[4] T. Yamaguchi, Y. Kurosawa and S. Matsumura, "FEA for damping of structures having elastic bodies, viscoelastic bodies, porous media and gas", ***Mechanical Systems and Signal Processing***, Vol.21, No.1, pp.535-552, 2007.

[5] T. Yamaguchi, Y. Nakamoto, Y. Kurosawa and S. Matsumura, "Dynamic analysis of dissipated energy for automotive sound-proof structures including elastic body, viscoelastic body and porous body using FEM in sound bridge phenomena", ***Journal of Environment and Engineering***, Vol.2, No.2, pp. 315-326, 2007.

[6] T. Yamaguchi, Y. Kurosawa and H. Enomoto, "Damped vibration analysis using finite element method with approximated modal damping for automotive double walls with a porous material", ***Journal of Sound and Vibration***, Vol.325, pp.436-450, 2009.

[7] H. Oberst, ***Akustische Beihefte*** , Helt 4, pp.181-194,1952.

[8] H. Utsuno, T. W. Wu, A. F. Seybert and T. Tanaka, "Prediction of sound fields in cavities with sound absorbing materials", ***AIAA Journal***, Vol.28, No.11, pp.1870-1875. 1990.

[9] O. C. Zienkierwicz and Y. K. Cheung, ***The Finite Element Method in Structural and Continuum Mechanics***, McGraw-Hill, 1967.